Ultra-elongated depth of focus of plasmonic lenses with concentric elliptical slits under Gaussian beam illumination*

Wang Jing(王 婧) and Fu Yong-Qi(付永启)†

School of Physical Electronics, University of Electronic Science and Technology of China, Chengdu 610054, *China*

(Received 27 December 2012; revised manuscript received 24 February 2013)

In this paper, we discuss the influence of ratio of minor to major axis on the propagation property and focusing performance of a plasmonic lens with variant periodic concentric elliptical slits illuminating under a Gaussian beam. In order to analyse the influence theoretically, a finite-difference time-domain (FDTD) numerical algorithm is adopted for the computational numerical calculation and the design of the plasmonic structure. The structure is flanked with penetrated slits through a 200-nm metal film (Au) which is coated on a quartz substrate. Tunability of focusing capability of the plasmonic lenses is studied by tailoring the ratio. Our calculation results demonstrate that the ratio of the elliptical slits greatly affects the focusing capability of the lense. The plasmonic lenses with concentric elliptical slits illuminating under a Gaussian beam have ultra-elongated depth of focus. These results are very encouraging for the future study of the plasmonic lens-based applications.

Keywords: ultra-elongated depth of focus, plasmonic lenses, elliptical slits, finite-difference time-domain

PACS: 02.70.–c, 41.20.Jb, 42.30.–d, 42.79.Bh **DOI:** 10.1088/1674-1056/22/9/090206

1. Introduction

Characteristics of surface plasmon polariton (SPP)-based nanophotonic devices are appealing to numerous researchers due to their extraordinary transmission in free space recently.[1–8] Lately, nanosandwich waveguide,[9] SPP-based superlens,[10] resonance immunosensors,[11] nanobiosensors,[12] and nanoprobes[13] were reported. Many functions can be realized using the reported SPP-based nanophotonic devices, such as superfocusing, detection, biosensing and collimating. It is found that extraordinary enhancement of transmission can be obtained by the interaction among SPPs. More recently, superfocusing especially the tight focusing in nanoscale confinement of SPP has been researched actively. Fu *et al.*[5–14] demonstrated that a silver film coated on glass with some corrugations can play a role as a superlens. Many other researchers have found the similar results.[15–18] It was reported that the optical resolution of the plasmonic structure can break through the diffraction limit.[19–21] However, the shape of the focal point is not ideal.

Lerman *et al.*[22] found a novel focusing phenomenon of a plasmonic lens with a single elliptical slit illuminated with radially polarized field. But the radially polarized light source is complicated in comparison with a Gaussian beam, and restricts the miniaturization of the optical system. Considering this, we put forth a plasmonic lens consisting of a total of eight concentric elliptical slits with varying periods under the illumination of a Gaussian beam as shown in Fig. 1. It consists of a total of eight elliptical rings thoroughly penetrating Au thin film. Focusing performance and propagation property can be modified by changing the ratio of semi-minor axis to semi-major axis of the elliptical slits. Our target is to study tunability of the focusing capability of the plasmonic lenses. Our calculation results demonstrate that the plasmonic lenses with concentric elliptical slits can realize the function of generating a focal point with ultra-elongated depth of focus under a Gaussian beam illumination of linear polarization. Furthermore, our lenses have a significant feature of ultra-elongated depth of focus which may be interesting for practical applications. It means that the focusing serving as feedback control system can be omitted in the systems for applications of data storage, nanolithography, medical monitoring, etc.

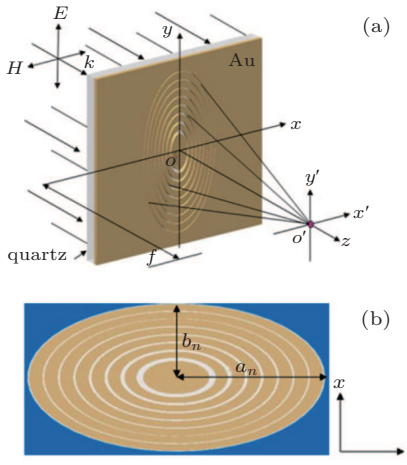


Fig. 1. (color online) (a) Schematic diagram of the plasmonic zone plate-like structure for super-focusing with focal length f. (b) Top view of the structure.

*Project supported by the National Natural Science Foundation of China (Grant Nos. 11079014 and 61077010).

†Corresponding author. E-mail: yqfu@uestc.edu.cn

© 2013 Chinese Physical Society and IOP Publishing Ltd

2. Structure construction and simulation setup

The plasmonic lenses proposed here are designed with a variant period calculated using the equation of the optical path difference as $b_n^2 = 2nf\lambda + n^2\lambda^2$, whereas n is the ring number, f the focal length ($f = 1\mu$m), b_n the inner semi-minor axis of the n-th elliptical slits, and λ the incident wavelength. The semi-major a_n is determined by the ratio (b_n/a_n) which is varied in a range from 0.4 to 0.9. The structure is composed of eight elliptical rings with an outer semi-minor axis of 5.144 μm in the case where the ratio is 0.8. The detailed values of the structure with a ratio of 0.8 are given in Table 1. The outer semi-minor B_n is determined by $B_n = b_n + w_n$ and the outer semi-major A_n is determined by the ratio (B_n/A_n). The value of the width between each slits (w_n) is calculated using the formula $w_n = \lambda f/2r_n$. Considering that the SPP effect is more effective for the noble materials, we select Au film with slits coated on a glass substrate. Dielectric constant at 532-nm wavelength is $\varepsilon_m = -5.63 + i2.21$ and $\varepsilon_d = 1.243$ for gold and glass, respectively. A Gaussian beam is added as a light source as shown in Fig. 1(a). The waist radius of the Gaussian beam is 1.02 μm and the light beam propagates along the z-direction. The mathematical expression for the incident wave is given below

$$E(r,z) = E_0(r,z)\frac{\omega_0}{\omega(z)}\exp\left[-\frac{r^2}{\omega^2(z)}\right] \times \exp\left\{-i\left[k\left(z+\frac{r^2}{2R(z)}\right)-\arctan\frac{z\lambda}{\pi\omega_0^2}\right]\right\}, \quad (1)$$

where r is the radial distance from the central axis of the beam, z is the axial distance from the beams narrowest point, i is the imaginary unit, $k = 2\pi/\lambda$ is the wave number, E_0 is the constant, $\omega(z)$ is the radius at which the field amplitude and intensity drop off to $1/e$ and $1/e^2$ of their axial values respectively, ω_0 is the waist radius, $R(z)$ is the radius of curvature of the beam wavefront. The vacuum wavelength of the incident light is $\lambda_0 = 532$ nm. An Au film of thickness $h = 200$ nm centred at $z = -100$ nm has a micro-zone plate-like structure embedded in the metal film. We investigate the SPP transmission mechanism by analysing the electromagnetic field distributions in the near-field of exit plane of the plasmonic lenses. The ratio of elliptical slits is used as a variable parameter to study the corresponding variations in the transmission and focusing performance of the lens. The FDTD algorithm is adopted in our numerical computational analyses (commercial software FDTD Solution bought from Lumerical Solution Inc. company, Canada). In the FDTD three-dimensional (3D) calculations, simulation time and mesh size are 50 fs, $\Delta x = 10$ nm, $\Delta y = 10$ nm, and $\Delta z = 10$ nm, respectively. Theoretically, the calculation result is acceptable as long as the mesh size is less than $\lambda/10$. The perfectly matched layer (PML) boundary condition is applied to the grid boundaries.

Table 1. Detailed values of the structure in the case of 0.8; a_n and b_n are the inner semi-minor axis and semi-major axis; A_n and B_n are the corresponding outer semi-minor axis and semi-major axis; w_n is the width between each slits.

Ring number	a_n/μm	b_n/μm	A_n/μm	B_n/μm	w_n/nm
$n = 1$	1.447	1.158	1.733	1.387	228.848
$n = 2$	2.251	1.801	2.435	1.948	147.141
$n = 3$	2.986	2.389	3.125	2.500	110.918
$n = 4$	3.693	2.955	3.806	3.045	89.666
$n = 5$	4.387	3.510	4.482	3.586	75.491
$n = 6$	5.073	4.059	5.155	4.124	65.293
$n = 7$	5.753	4.603	5.825	4.660	57.576
$n = 8$	6.430	5.144	6.493	5.195	51.519

3. Results and discussion

Figures 2(a)–2(f) show the electric-field intensity distributions in the x–z plane for the case of ratio varying in a range from 0.4 to 0.9, illuminating under a Gaussian beam. Figures 2(g)–2(l) show the corresponding electric field intensity distributions in the y–z plane. Focusing capability appears in the case of ratio = 0.6. However, the focusing is not ideal. The intensity of the focusing is weak and even the intensities of the sidelobes are stronger than that of the mainlobe. The intensity of the focusing increases when the ratio rises to 0.7 and the focusing becomes best in the cases of ratio = 0.8 and ratio = 0.9. This phenomenon can be explained as the fact that the plasmonic lenses with slits couple incident light together with the SPP waves. The SPP waves are excited on one side of the interface by direct light illumination via slits coupling, tunnel through the film, and be re-emitted on the other side.[23] The lens with variant periodic concentric elliptical slits acts as an antenna to couple incident light into SPPs. As a consequence the electromagnetic fields at the surface become intense above the lens[24] and then SPPs interfere with diffractive wavelets from the slits and form a finely focal point in ultra-elongated size after exit plane in free space. Figure 3 shows electron-field (E-field) intensity distributions in the x–y plane ($z = 0.1$ μm, exit plane in free space). The shape of the focal point is elliptical. What we are most concerned about are two parameters in superfocusing: depth of focus (DOF) which measures the tolerance of placement of the image plane in relation to the lens and the largest focusing spot size of the beam at the site of full width and half maximum (FWHM). Figures 2 and 3 show the propagation properties and focusing

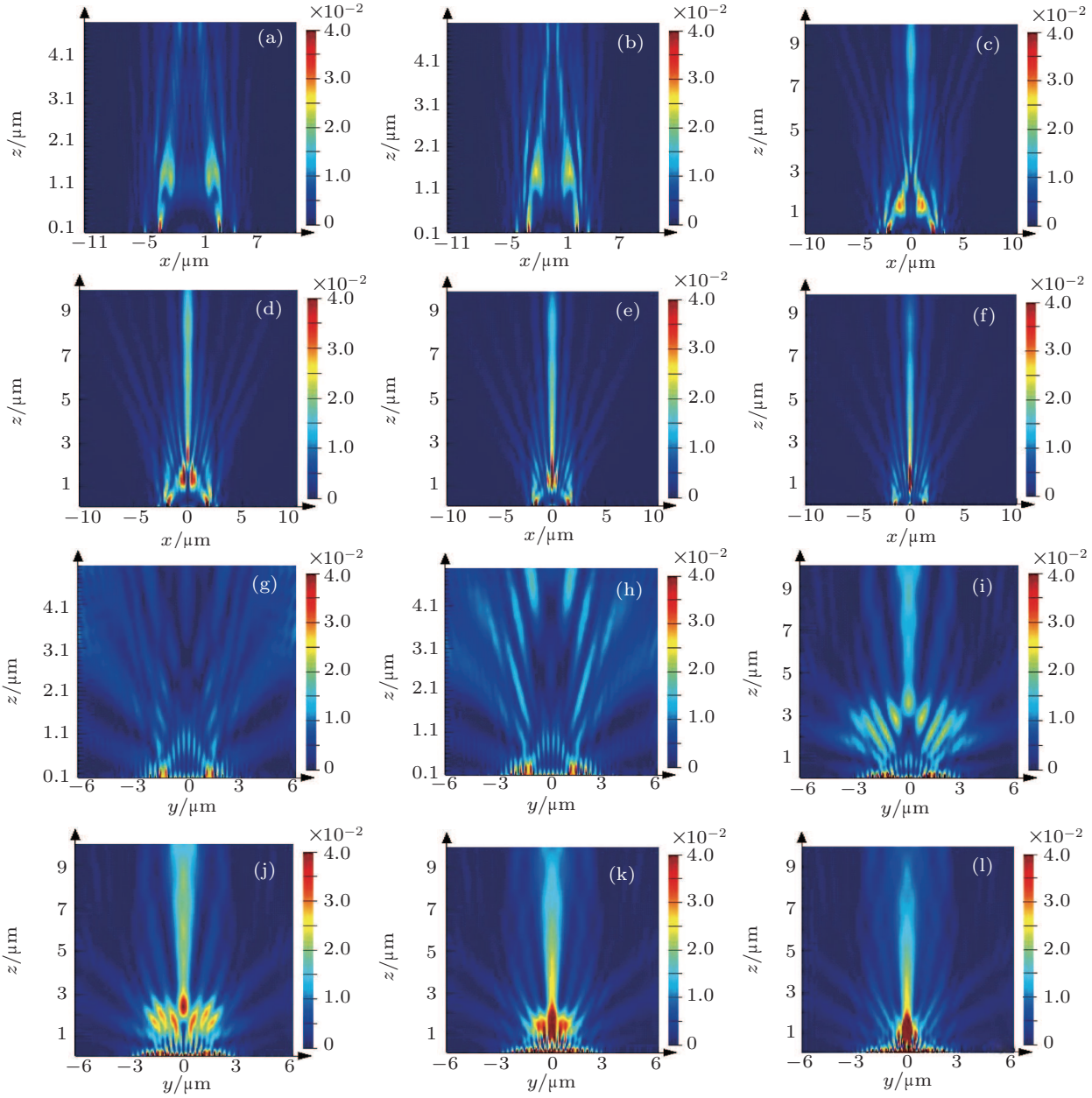


Fig. 2. (color online) E-field intensity distributions under Gaussian beam illumination for ratios varying from 0.4, 0.5, 0.6, 0.7, 0.8, to 0.9 (a)–(f) in the x–z plane; (g)–(l) in the y–z plane.

performances in the case of varying ratio under a Gaussian beam illumination. It can be seen that the most exciting point is that the plasmonic lens with concentric elliptical slits under a Gaussian beam illumination has an ultra-elongated depth of focus. It can be seen apparently from Figs. 2(d) and 2(j) that the DOF is almost 8 μm for ratio = 0.7 and DOF of the lens even extends up to 9 μm for ratio = 0.8 as shown in Figs. 2(e) and 2(k). Obviously, the DOF of the lens for ratio = 0.9 is shorter than the DOF for ratio = 0.8. The focusing beam of light is converged which is not emanative. The long and elongated DOF is of important significance in imaging and applications in nanoscale microscopy. It is interesting that the beam propagation is varied for the Gaussian beam illumination with the ratio increasing. Here, the ratio which can change the curvature of the elliptical silts largely influences the DOF. The beam in free space is divided into two beams in the central region along the z axis for the cases of ratio = 0.4, 0.5, and merged into one beam for the cases of ratio = 0.6, 0.7, 0.8, and 0.9. Apparently, the different ratios strongly influence the size of the focal point. Fu *et al.*[5] and Shankaran *et al.*[11] reported that a plasmonic micro-zone plate-like metallic structure with circular variant periods can realize superfocusing in propagation direction at a quasi-far filed region ($\lambda \sim 5\lambda$), at a working wavelength of 633 nm, the focal spot of the plasmonic lens is 210 nm at site of full width half maximum (FWHM) in the y direction and 250 nm in the x direction under the assumption of the illumination under linear y polarization. Of course, the lens with elliptical slits has a longer DOF than the lens with circular slits. More details can be found in Refs. [5]

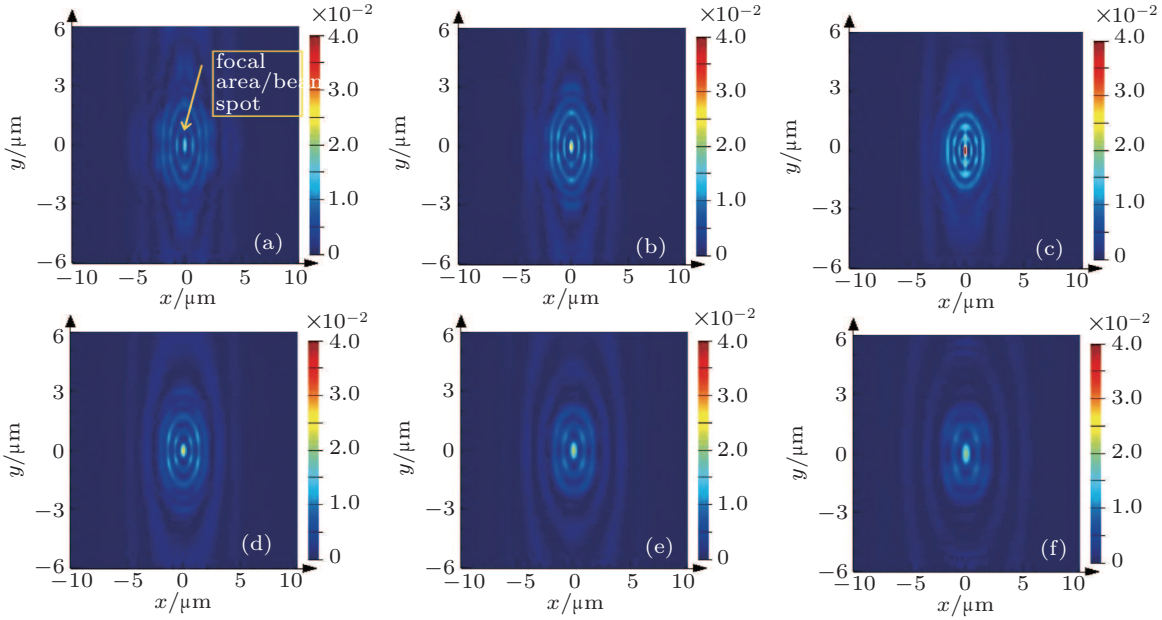


Fig. 3. (color online) E-field intensity distribution at $x-y$ plane ($z = 0.1$ μm, exit plane in free space). (a) E-field intensity distribution at x–y plane, $z = 4$ μm for ratio = 0.6; (b) E-field intensity distribution at x–y plane, $z = 3$ μm for ratio = 0.7; E-field intensity distribution at x–y plane, for ratio = 0.8 (c) $z = 2$ μm, (d) $z = 3$ μm, (e) $z = 4$ μm, (f) $z = 5$ μm.

and [11]. In order to compare the focusing properties, the relevant results are shown in Fig. 4. After comparison we can draw a conclusion that the capability of focusing for the ratio = 0.8 is much better than for the ratio = 0.6 and 0.7 in the sense of either the intensity or the FWHM. FWHM varies with position of plane. The two-dimensional (2D) profile of the electric intensity versus the position at x and y axes with the largest width of the focusing beam in the case of ratio=0.8 are shown in Figs. 5(a) and 5(b). It can be seen from Fig. 5(a) that the FWHM of the structure approaches the diffraction limit at x direction and the intensity of the main lobe is much stronger than those of the nearby sidelobes. To further investigate the focusing capability, we plot the phase distributions for the case of ratio = 0.8, $z = 2$ μm under a Gaussian beam illumination in (a) x–y plane, (b) x–z plane, and (c) y–z plane, respectively. Figure 6 shows phase distributions of the beam propagation after the exit plane in free space. As can be seen, the phase is delayed along the long-axis. The interference between ±1 diffraction orders makes a significant contribution to the focusing. The field distributions will be much different after the exit plane when the Gaussian beams are changed into plane waves. The further study of the plane wave illumination will be carried out very soon.

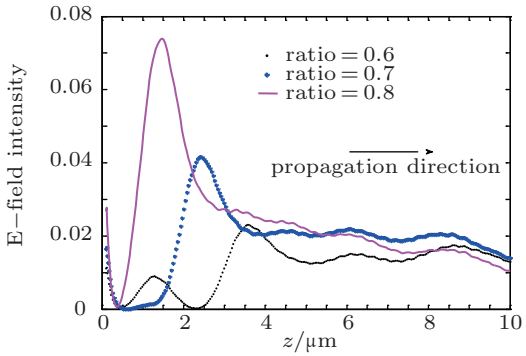


Fig. 4. (color online) The 2D profiles of E-field intensity distribution under Gaussian beam illumination in direction of propagation for ratio = 0.6, 0.7, and 0.8. Each peak represents a focusing area.

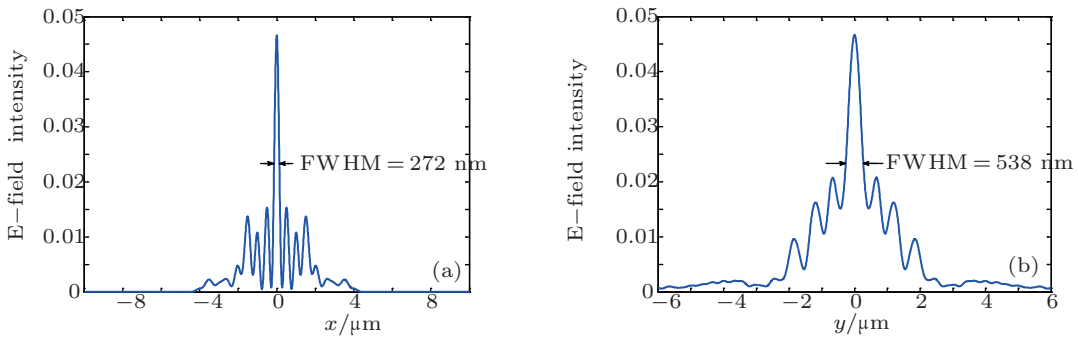


Fig. 5. (color online) The 2D profiles of E-field intensity distribution for case of ratio = 0.8 under a Gaussian beam illumination at propagation distance $z = 2$ μm (a) in the x axis and (b) in the y axis.

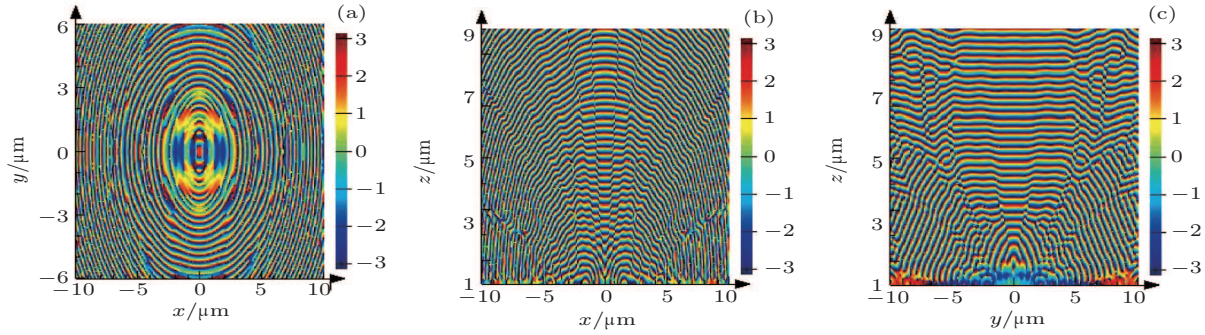


Fig. 6. (color online) Phase distributions for the case of ratio = 0.8, $z = 2$ μm under a Gaussian beam illumination (a) in the x–y plane, (b) in the x–z plane, and (c) in the y–z plane.

4. Summary

In the present paper, we discuss the different-ratio propagation properties and focusing performance of a plasmonic lens with variant period concentric elliptical slits. Our computational calculation results demonstrate that the propagation properties and focusing performance are mainly influenced by the ratio of the elliptical slits etched on the Au thin film coated on the glass. For the ratios ranging from 0.6 to 0.9, focusing in free space can be obtained. An excellent focusing capability can be formed for the case of ratio = 0.8. For the lenses with the ratios of 0.4 and 0.5, nearly no focusing region can be formed due to large slit width so that it is too large to diffract the incident beam, and no interference occurs in free space accordingly. The plasmonic lenses with concentric elliptical slits illuminating under Gaussian beam have ultra-elongated DOF as long as 9 μm. For some specific applications such as nano-photolithography, the long working distance is a crucial issue. The propagation property and focusing performance are sensitive to the ratio of the elliptical slits.

References

[1] Barnes W L, Dereux A and Ebbesen T W 2003 *Nature* **424** 824

[2] Martin-Moreno L, Garcia-Vidal F J, Lezec H J, Pellerin K M, Thio T, Pendry J B and Ebbesen T W 2001 *Phys. Rev. Lett* **86** 1114

[3] Levy U, Abashin M, Ikeda K, Krishnamoorthy A, Cunningham J and Fainman Y 2007 *Phys. Rev. Lett.* **98** 243901

[4] Ebbesen T W, Lezec H J, Ghaemi H F, Thio T and Wolff P A 1988 *Nature* **391** 667

[5] Fu Y Q, Zhou W and Lim L E N 2008 *J. Opt. Soc. Am. A* **25** 238

[6] Fu Y Q, Zhou X L and Zhao W 2009 *J. Comput. Theor. Nano* **6** 617

[7] Liang G F, Zhao Q, Chen X, Wang C T, Zhao Z Y and Luo X G 2012 *Acta Phys. Sin.* **61** 104203 (in Chinese)

[8] Zhong R B, Liu W H, Zhou J and Liu S G 2012 *Chin. Phys. B* **21** 117303

[9] Ya F Y, Zhou W J, Liu A J, Chen W, Wang Y F, Yan X Y and Zheng W H 2011 *Chin. Phys. B* **20** 087301

[10] Lee H, Xiong Y, Fang N, Srituravanich W, Durant S, Ambati M, Sun C and Zhang X 2005 *New J. Phys.* **7** 255

[11] Shankaran D R, Gobi K V and Miura N 2007 *Sens. Actuators B* **121** 158

[12] Pumera M, Sánchez S, Ichinose I and Tang J 2007 *Sens. Actuators B* **123** 1195

[13] Descrovi E, Vaccaro L, Nakagawa W, Aeschimann L, Staufer U and Herzig H P 2004 *Appl. Phys. Lett.* **85** 5340

[14] Fu Y Q, Zhou W, Lim L E N, Du C L and Luo X G 2007 *Appl. Phys. Lett.* **91** 061124

[15] Lerman G M, Yanai A and Levy U 2009 *Nano Lett.* **9** 2139

[16] Shi H F, Wang C T, Du C L, Luo X G, Dong X C and Gao H T 2006 *Opt. Express* **13** 6815

[17] Kim S, Lim Y, Kim H, Park J and Lee B 2008 *Appl. Phys. Lett.* **92** 013103

[18] Kim H C, Ko H and Cheng M 2009 *Opt. Express* **17** 3078

[19] Fang Z Y, Lin C F, Ma R M, Huang S and Zhu X 2010 *ACS Nano* **4** 75

[20] Neacsu C C, Berweger S, Olmon R L, Saraf L V, Ropers C and Raschke M B 2010 *Nano Lett.* **10** 592

[21] Lin L, Xiao M G, McGuinness L P and Roberts A 2010 *Nano Lett.* **10** 1936

[22] Lerman G M, Yanai A, Ben-Yosef N and Levy U 2010 *Opt. Express* **18** 10871

[23] Maier S 2007 *Plasmonics: Fundamentals and Applications* (New York: Springer) p. 158

[24] Genet C and Ebbesen T W 2007 *Nature* **445** 39